Journal of the European Ceramic Society **19** (1999) 2833–2841

PII: S0955-2219(99)00071-0
0955-2219/99/$ - see front matter

Formation of Nanometric Hard Materials by Cold Milling

N. J. Welham [ab]* and D. J. Llewellyn [ac]

[a]Department of Electronic Materials Engineering, Research School of Physical Sciences and Engineering, Australian National University, Canberra, ACT 0200, Australia
[b]Department of Applied Mathematics, Research School of Physical Sciences and Engineering, Australian National University, Canberra, ACT 0200, Australia
[c]Electron Microscopy Unit, Research School of Biological Sciences, Australian National University, Canberra, ACT 0200, Australia

(Received 31 December 1998; accepted 13 March 1999)

Abstract

The fabrication of nanosized, single crystal TiC or TiN powders from ilmenite or TiO_2 within a single low temperature stage is reported in this paper. The titaniferous powders were ball milled for 100 h in a laboratory scale mill with magnesium powder and either graphite or nitrogen. The resultant powders were then subjected to an annealing step at 1200°C. Differential thermal analysis and X-ray diffraction showed that the phases formed within the milling step and underwent grain growth on annealing. Acid leaching of the powders selectively removed the unwanted product phases leaving only the hard material. The final particle size and Scherrer XRD crystallite size were similar after annealing, implying that the particles produced were single crystal.

Keywords: TiC, TiN, TiO_2, powders-solid state reaction, milling.

1 Introduction

There is great interest in the formation of nanosize particles due to their unusual properties. Conventional mechanical processing eventually leads to nanocrystalline or amorphous materials, these powders typically possess particle sizes of 100–1000 nm. There is an equilibrium between breakage and rewelding of powders giving a constant particle size, although these grains are agglomerates of smaller particles.[1–4]

It has recently been shown that mechanochemical processing can produce metallic particles of 100 mn and smaller.[5–8] The formation of nanosized compounds is also of great interest in many fields where the properties are closer to the theoretical than to the measured bulk, e.g. in quantum dots.[9] Nanometric particles of ZrO_2[10] and alumina[11] have also been produced by mechanochemical reaction, but these have required thermal treatment for the reactions to occur. Thus far, the reactions producing nanometric particles have been comparatively simple using two reactants during either metallic reduction or displacement reactions.

Previous papers have examined the formation of titanium nitride,[12] carbide[13] and carbonitride[14] from rutile and ilmenite by reduction with aluminium in the presence of nitrogen and/or graphite. The reactions were shown to be complete after milling with the formation of nanostructured micronised particles containing alumina, the titanium bearing hard phase and iron.[15]

In this paper a similar reaction process is utilised as before[12–14] but using magnesium, which forms a soluble oxide, as the reductant in place of aluminium. A thermal processing step giving crystallite growth, either before or after separation from the other products, would possibly lead to defect-free nanometric single crystals of hard materials. These particles may prove to be of great importance, due to the increased resistance to impact breakage of single crystals compared with polycrystalline materials, possibly leading to a new generation of hard material products.

* To whom correspondence should be addressed. Fax: +61-2-6249-0511; e-mail: nicholas.welham@anu.edu.au

2 Experimental

The titaniferous feed powders consisted of ilmenite and rutile. The ilmenite was obtained from a commercial concentrator of natural beach sands and was >96 wt% $FeTiO_3$, the main impurities being Mn, Zr and Si. The grains were rounded, as is typical of ilmenite derived from beach sands and had $d_{50} = 150\,\mu m$. Optical microscopy indicated that zircon ($ZrSiO_4$) was also present and was the major mineral impurity. The rutile was pigment grade material from a commercial chloride route processing plant. X-ray fluorescence analysis of the powder showed it was >99.9 wt% TiO_2 with no Zr, Al or Si (whose oxides are common coatings for pigment TiO_2) present. X-ray diffraction (XRD) of the powder showed it to be mainly the rutile crystalline form with a small fraction of anatase (estimated from relative peak areas on the XRD trace at 1–2%). The particle size was 0.22–0.26 μm.

The magnesium and graphite powders were both nominally >99 wt% and had particle sizes of $<50\,\mu m$, the magnesium particles were irregular in shape and the graphite flaky. The nitrogen used was 99.9%. Feed powders were prepared in accordance with the stoichiometry of reaction eqns (1)–(4), which were the thermodynamically predicted reactions.[16]

$$TiO_2 + 2Mg + C \Rightarrow TiC + 2MgO \quad (1)$$

$$FeTiO_3 + 3Mg + C \Rightarrow Fe + TiC + 3MgO \quad (2)$$

$$2TiO_2 + 4Mg + N_2 \Rightarrow 2TiN + 4MgO \quad (3)$$

$$2FeTiO_3 + 6Mg + N_2 \Rightarrow 2TiN + 6MgO + 2Fe \quad (4)$$

Seven grammes of each mixture was placed in a laboratory scale tumbling ball mill made of 316 stainless steel, as previously described.[17] Five 1 inch (25·4 mm) diameter 420C stainless steel balls were used giving a ball:powder mass ratio of 43:1, the mill was rotated at 165 rpm for 100 h. The mills were evacuated to $\sim 10^{-2}$ Pa and those running (3) and (4) were backfilled with nitrogen to 500 kPa. The pressure was maintained at >400 kPa by adding nitrogen as necessary to account for consumption or leakage.

Differential thermal analysis (DTA) was performed on selected powders using approximately 20 mg; samples were heated up in a recrystallised alumina crucible under an argon atmosphere to 1200°C at a heating rate of 20°C min^{-1} using a Shimadzu DTA-50 instrument. Thermogravimetric analysis (TGA) was also performed using the same parameters in a Shimadzu TGA-50. After heating to 1200°C, the samples were cooled to <1000°C within 1 min and then more slowly to room temperature. Milled powders were also annealed under flowing argon for 1 h at 1200°C.

Agitated leaching of the products was performed for 18 h at room temperature using 3% HCl at a slurry density of 1 w/v. This leachant was chosen as it readily reacts with the unwanted products—elemental iron and MgO. Powders were leached both before and after annealing for 1 h at 1200°C, to determine the most efficient method of separation of the hard material particles from the unwanted matrix.

The products were analysed by X-ray diffraction (XRD) using monochromatic Co K_α radiation ($\lambda = 0{\cdot}178896$ nm) with a count time of 2 s per 0·02° step. Crystallite size was calculated from the fitted peak widths using Scherrer's formula.[18] The subscripted numbers in Table 1 are the 2σ values calculated from the variation in the individual peaks. No data could be calculated for the unleached, unannealed powders due to excessive overlap between the peaks of the hard material and MgO. The crystallite sizes for MgO in the annealed samples were derived from only two peaks, consequently no standard deviation was calculated. The unit cell size was determined from the relationship between the unit cell parameter and the measured d-spacings.[19]

Transmission electron microscopy (TEM) was performed on the powders obtained after leaching of both as-milled and annealed powder. The powders were dispersed in ethanol and drops of the resultant suspension were placed onto holey carbon grids and allowed to evaporate. Bright field images and selected area electron diffraction patterns (SADP) were obtained using a Jeol 200CX TEM operating at 200 keV.

3 Results

3.1 Thermal analysis

DTA on the as-milled powders showed there were no thermal events up to 1200°C. Previous work on this system in the absence of carbon or nitrogen[20] has shown that the reaction of a physical mixture occurs at around 600°C—below the melting point of magnesium. The reaction was highly exothermic and may have been accelerated by the melting of magnesium within the volume surrounding the centres of reaction causing an increased interfacial surface area between reactants in the solid-state process. Clearly, the absence of thermal events implies that the reaction had been completed

Table 1. Post-leaching crystallite sizes and calculated unit cell sizes for TiC/TiN of the as-milled and annealed powders

	Crystallite size (nm)				*Unit cell size (nm)*		
	As-milled	*Annealed*			*As-milled*	*Annealed*	
System	*Leached*	*Unleached*	*Leached*	*MgO*	*Leached*	*Unleached*	*Leached*
TiO_2+C	$7{\cdot}6_{5{\cdot}3}$	$16{\cdot}5_{0{\cdot}4}$	$17{\cdot}4_{2{\cdot}0}$	33	$0{\cdot}4273_{36}$	$0{\cdot}4276_{5}$	$0{\cdot}4280_{3}$
$FeTiO_3+C$	$5{\cdot}3_{3{\cdot}3}$	$8{\cdot}9_{1{\cdot}7}$	$10{\cdot}2_{2{\cdot}0}$	23	$0{\cdot}4260_{15}$	$0{\cdot}4305_{7}$	$0{\cdot}4316_{12}$
TiO_2+N_2	$5{\cdot}5_{1{\cdot}9}$	$19{\cdot}0_{3{\cdot}1}$	$19{\cdot}8_{3{\cdot}3}$	34	$0{\cdot}4230_{15}$	$0{\cdot}4234_{4}$	$0{\cdot}4244_{4}$
$FeTiO_3+N_2$	$7{\cdot}6_{4{\cdot}4}$	$17{\cdot}8_{1{\cdot}3}$	$20{\cdot}2_{3{\cdot}4}$	21	$0{\cdot}4230_{6}$	$0{\cdot}4239_{8}$	$0{\cdot}4243_{3}$

within the mill. TGA of the milled powders showed no change in mass, confirming the reactions were entirely solid-state. The absence of a mass loss showed that the carbon in the system had been fixed during milling or carbothermic reduction of ilmenite or rutile would have occurred at temperatures in excess of 700°C.[21–28] For the nitrogen system there was no change in mass, confirming that any nitrogenous phases within the system formed during milling.

3.2 X-ray diffraction

X-ray diffraction traces of the as-milled powders are shown in Fig. 1. It is clear that in all cases MgO is the predominant phase present, although rutile remains in (a) and iron is probably present in (b), (c) and (d). The iron in (c) is due to abrasion from the balls and mill whereas that in (b) and (d) is from reduction of the ilmenite. The broadness of the MgO peaks is such that evidence for the hard material phases is inconclusive, although there seems to be a shoulder on the main peak in traces (a) and (b) that are probably due to TiC. The peaks for MgO and TiN are separated by $<0{\cdot}4°$ which is less than the fitted peak width of $>1{\cdot}5°$. This, coupled with the low intensity of TiN peaks directly after formation during milling,[12,25] make it probable that any TiN peaks present are overlaid by the stronger MgO peaks. Crystallite sizes cannot be calculated for any phases in these as-milled powders due to overlap of the peaks for TiC and TiN by the MgO peaks.

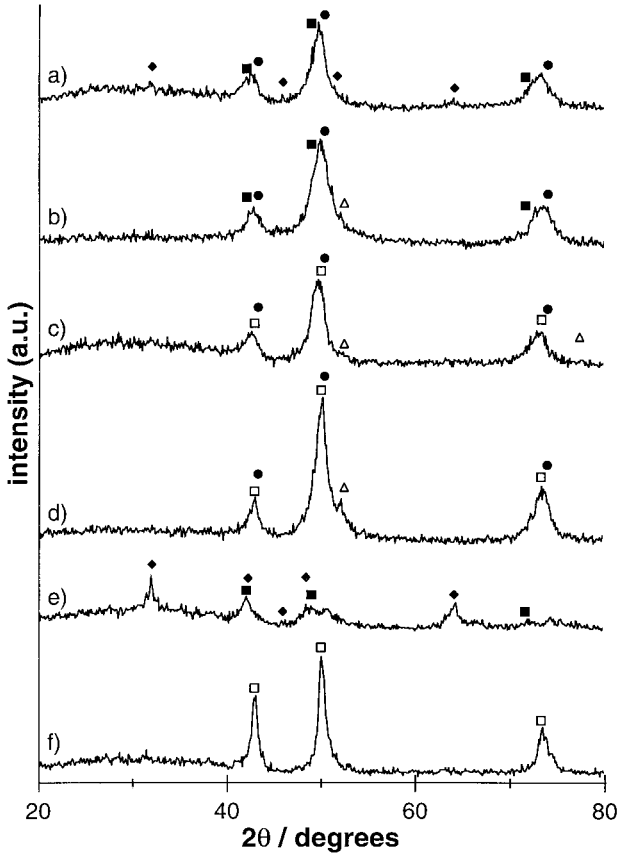

Fig. 1. Intensity: 2θ traces for (a), (b), (c) and (d) as-milled powders for reactions (1)–(4), respectively; (e) and (f) reactions (1) and (4) after 18 h in 3% HCl at room temperature. ●, MgO; ■, TiC; □, TiN; ◆, TiO_2; △, Fe.

The powders were annealed under argon for 1 h at 1200°C and the XRD traces for these powders are shown in Fig. 2. Clearly, there has been significant grain growth resulting in the narrowing of peaks and the emergence of hitherto unobserved phases. The peaks for titanium carbide are still incorporated with the MgO peaks which suggests that the crystallisation of MgO is either more rapid than TiC or hinders the growth of TiC. There is some separation of the TiC and MgO peaks at high angles, although the TiC peaks are still relatively weak compared with the MgO peaks. For rutile milled with carbon (a) no other phases are evident implying that reaction (1) was complete and was not subject to a further thermal reaction. The absence of either the exotherm for reduction of TiO_2 observed previously[20] or the melting of residual Mg would seem to confirm the completion of reaction during milling.

The peaks for TiC are all at slightly higher 2θ than the standard peaks for TiC. The position of the peaks are a function of the carbon content[29,30] and the carbide was estimated to be $TiC_{0{\cdot}5}$, which is as carbon deficient as possible.[29,30] However, an oxycarbide phase of the general formula TiC_xO_{1-x}, has been observed during the carbothermic reduction of both rutile[31–33] and ilmenite[34,35] and may well be present here. This phase has a smaller unit cell than TiC and therefore shows XRD peaks at slightly higher angles, as observed here. It has been shown[29,34,35] that

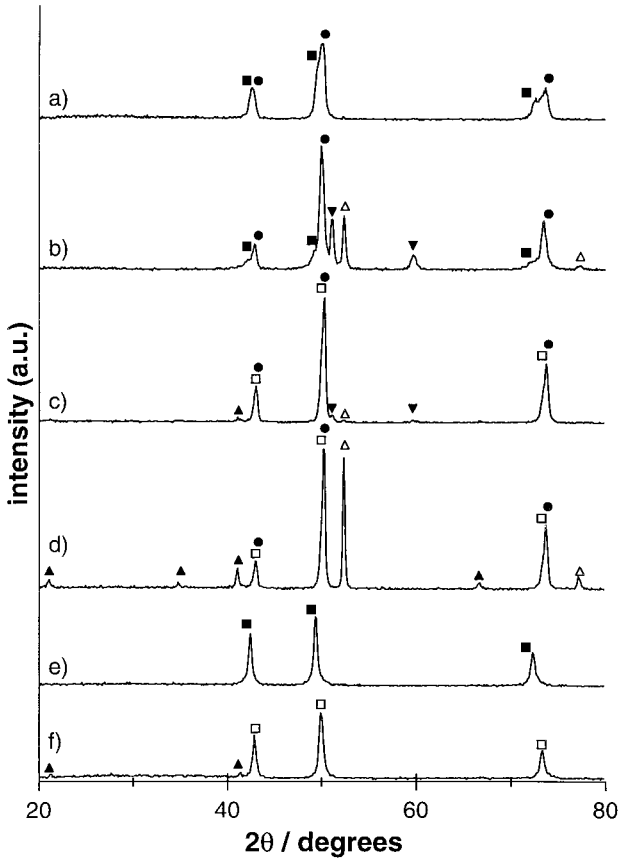

Fig. 2. Intensity: 2θ traces for (a), (b), (c) and (d) powders for reactions (1)–(4) after annealing under argon at 1200°C for 1 h; (e) and (f) annealed powders for reactions (1) and (4) after 18 h in 3% HCl at room temperature. ●, MgO; ■, TiC; □, TiN; △, Fe; ▲, $MgTi_2O_4$; ▼, Fe(C).

the removal of small fractions of oxygen from the oxycarbide phase is difficult, but can be achieved by increasing the annealing temperature.[29,34] Thus, the ambient temperature reaction which occurred during milling would more probably result in an oxycarbide phase than a carbon deficient carbide, the unit cell for the phase is equivalent to $TiC_{0.66}O_{0.34}$, assuming Vegards law applies.

For ilmenite, trace (b), the MgO peaks are clearly visible and the oxycarbide peaks are much smaller but somewhat wider, making them more evident than in trace (a). Peaks for iron and a solid solution of carbon in iron are evident, as would be expected from the significant iron content of ilmenite. The incorporation of some carbon into the iron would imply that the titanium phase formed was carbon poor. From the calculated unit cell size (Table 1), the cubic phase was estimated to be either $TiC_{0.54}$ or, more probably, $TiC_{0.85}O_{0.15}$.

The two nitride samples (c) and (d) show peaks for MgO, iron and a new phase, $MgTi_2O_4$. The peaks for TiN are overlapped by the stronger peaks of MgO and are not obvious, although profile fitting confirmed that two peaks were present. There is some slight contamination by iron in the rutile sample (c) due to abrasion from the mill and balls, presumably the contamination in the other samples was too small to detect by XRD.

The formation of $MgTi_2O_4$ may have occurred during milling or annealing, there were no peaks evident directly after milling which may imply that it was due to a thermally induced reaction. The absence of thermal events during DTA neither confirms or contradicts the two possible mechanisms of formation. Earlier work on the mechanochemically induced magnesium reduction of rutile[20] showed the formation of $MgTi_2O_5$ during annealing—the solid-state reaction between TiO_2 and MgO becoming more extensive with increasing time and temperature. An analogous reaction may be occurring in this system, however, the absence of $MgTi_2O_5$ after annealing seems to suggest that the reduction of TiO_2 to lower valence oxides of the general formula Ti_nO_{2n-1} occurs prior to magnesium incorporation.

$$Mg + 2TiO_2 \Rightarrow MgO + Ti_2O_3$$
$$\Rightarrow MgTi_2O_4 \qquad (5)$$

The absence of a peak in the DTA trace would seem to discount the first step occurring thermally as it has an enthalpy of $-230\,kJ\,mol^{-1}$ Mg, although it may simply be too slow to detect by DTA. Thus, it seems that the first stage occurs during milling, but whether the second stage occurs during milling or annealing is uncertain. No thermodynamic data is available for the $MgTi_2O_4$ phase, but similar reactions involving Fe_2O_3, Cr_2O_3 and $A1_2O_3$ all show favourable free energies (-17 to $-36\,kJ\,mol^{-1}$) indicating that formation during milling is probably feasible.

The unit cell size of TiN was determined from the profile fitted peak positions to be close to the accepted value of 0·424173 nm,[36] as shown in Table 1.

3.3 Separation

As-milled samples were leached and their XRD traces are shown in Fig. 1(e) and (f). Clearly, there are significant changes from the unleached powders (a) and (d) with the removal of the broad MgO and Fe peaks. Several peaks for rutile became apparent in (e) indicating that the reaction was incomplete after milling, whereas no new peaks were evident for the ilmenite sample (f). The absence of peaks for magnesium bearing phases would seem to suggest that aerial oxidation of the remaining elemental Mg had occurred on opening the mill to atmosphere. Confirmation of the presence of a TiC phase in (a) can be made due to clear separation from the now absent MgO, although there is some overlap with residual rutile peaks. The rutile peak around 31° has smaller satellite peaks around it;

these peaks are typical of incompletely reduced rutile where Ti_nO_{2n-1} phases are present.[25–28,37] The compositions of the insoluble phase formed from rutile and ilmenite were determined from the unit cell size (Table 1), to be $TiC_{0.39}$ and $TiC_{0.35}$, respectively. These values are substantially smaller than the most carbon deficient carbide reported, $TiC_{0.5}$[29,30] and confirm that the phase formed during milling was an oxycarbide, the composition of which was $TiC_{0.64}O_{0.36}$ and $TiC_{0.55}O_{0.45}$ for rutile and ilmenite, respectively.

The TiN derived from ilmenite (f) shows peaks which are narrower than those in (d) and have shifted to lower angles (i.e. greater d-spacings), as expected from the larger unit cell of TiN (0·424173 nm) compared with that of MgO (0·4213 nm).

The continued presence of rutile in (a) and the absence of reactant peaks in (f) would seem to imply that the reaction of ilmenite is more facile than that of rutile. It may be that the presence of iron enhances the reaction to form hard materials. In the carbothermal reduction of ilmenite and rutile it has been shown that, although the initial TiO_2 reduction reaction was unaffected by the presence of iron there was a clear enhancement of the latter stages of reduction due to the presence of iron.[20] This effect was attributed to an increase in the supply of carbon to the reaction interface by transport through the intimately mixed iron.

After leaching the samples annealed at 1200°C, the XRD traces shown in Fig. 2(e) and (f) were obtained. The leaching process has removed all of the iron and magnesium oxide as expected, although the $MgTi_2O_4$ phase is still present in the nitride sample derived from ilmenite (f).

The theoretical and experimental mass losses during leaching are shown in Table 2. Clearly, the mass losses during leaching of all of the as-milled powders were considerably greater than that predicted from the stoichiometry of reactions (1)–(4). This was not unexpected, it has been shown elsewhere that small crystallites formed during milling dissolve more rapidly than larger crystallites of the same material.[1–4,38,39] Indeed, this effect is evident here with an increase in crystallite size evident after leaching the annealed powders (Table 1). Dissolution in excess of the theoretical amount would indicate that titanium was solubilising in addition to the MgO (and Fe) which are both soluble in the acid used.

Table 2. Theoretical and experimental solubilities of reactions (1)–(4) before and after annealing for 1 h at 1200°C

System	*Theoretical*	*As-milled*	*Annealed*
$TiO_2 + C$	57·4	75·9	58·2
$FeTiO_3 + C$	56·6	91·5	64·5
$TiO_2 + N_2$	74·7	97·1	65·0
$FeTiO_3 + N_2$	74·1	96·6	82·2

The annealed powders showed less solubility than the unannealed powders, clearly the increased crystallite size hindered the dissolution process. The crystallite sizes of the TiC/TiN phases (Table 2), are clearly much larger for the annealed powders than the as-milled. However, the extent of dissolution was still greater than that predicted, for all except reaction (3), although there was no XRD evidence of phases other than TiN being present and the identity of the insoluble phase is unknown at present. The absence of TiO_2 in the leach product, although it was present before thermal treatment, could imply that the insoluble phase was a partially reduced titanium oxide. The absence of peaks for these phases may be due to a lack of crystallinity, or the presence of numerous intermediate phases which are insufficiently crystalline or abundant to detect. Leaching of the products of carbothermic reduction of rutile[37] has indicated that these titanium oxides are not particularly soluble in the solution used. Previous work on the magnesium reduction of ilmenite and rutile[20] has shown that TiO is probably formed during reaction, this phase is soluble in water and may well be the reason for the higher than expected solubilities.

For all carbide samples the unit cell size increased slightly after leaching (Table 1), which would seem to indicate that a low carbon content oxycarbide was more soluble than a high carbon oxycarbide phase. This is reasonable, assuming that TiC_xO_{1-x} has properties intermediate between those of highly soluble TiO and insoluble TiC.

There is also a slight increase in the nitride unit cell sizes after leaching. Although, titanium forms oxynitride phases, TiN_xO_{1-x}, they have only been reported during oxidation of TiN films[40,41] and not during reductive formation of TiN from TiO_2.[25–28,37] For the nitride the apparent increase in unit cell size is accompanied by a decrease in the data error due to peak fitting not correctly deconvoluting the TiN and MgO peaks in the annealed but unleached samples [Fig. 2(c) and (d)].

It should be noted that the calculated crystallite sizes for the unannealed rutile powders are based on fitting of the peaks which significantly overlap those of rutile. Thus, the value presented is probably as good an estimate of the rutile crystallite size as for the carbide/nitride. The crystallite sizes of the phases derived from ilmenite do not seem to be affected by the presence of other phases and can be considered reasonably reliable. Previous work[15] has indicated that titanium carbide/nitride derived thermally from rutile is generally of smaller crystallite size than that obtained from ilmenite under identical conditions and this may well be the case

here too. A higher quality XRD data set for samples of leached powders derived from rutile (0.02° step with a 20 s count time) did not enable the peaks for TiC_xO_{1-x}/TiN and TiO_2 to be resolved due to their similar d-spacings and the breadth of the fitted peaks.

3.4 Transmission electron microscopy

After 5 s sonication in ethanol in an ultrasonic bath the samples were observed to turn black and did not show signs of settling even after 1 h. Clearly, sonication is breaking up the powder into the component particles. Previous milling in a single phase system[1,4] has shown that sonication did not break up the aggregates observed by SEM. Thus, the presence of MgO must have prevented substantial rewelding of the hard material particles allowing the formation of separate particles.

Micrographs of several leached powders comprising oxycarbide and nitride powders derived from rutile and ilmenite, are shown in Fig. 3. The unannealed samples (a) and (b) clearly show smaller particles than the annealed samples (c) and (d); this is not unexpected as coalescence and growth can be expected to occur during annealing. This indicates that the individual hard material particles were not completely dispersed within the MgO (and iron) but were in contact. The sizes of particles in the unannealed powders were typically 3–14 nm, this range covers the 5–6 nm derived from XRD. The SADP of the as-milled powders (a) and (b) shows broad diffuse rings with few spots; this pattern is typical of material which contains a few large crystallites within an amorphous matrix. The Scherrer equation reports an average crystallite size[18] and a value within the range of measured sizes could be expected in this instance.

After annealing, the measured particle sizes were 11–21 and 3–36 nm for (c) and (d), respectively, the XRD crystallite sizes for these powders (Table 1), (17.4 and 20.2 mn) are within these ranges. The SADP for these powders show much narrower rings and more spots than the unannealed powders clearly indicating the presence of larger crystallites and a low content of amorphous material.

4 Discussion

The post-annealing XRD crystallite size of the MgO (Table 1) was somewhat larger than the size of the hard materials. In general, crystallite growth of phases increases as the annealing temperature approaches the melting point of the phase. In this system, the mp of MgO (2852°C) is similar to that of TiN (2930°C) but slightly smaller than that of TiC (3140°C), thus crystallite growth for MgO and TiN could be expected to occur at a similar rate with TiC slower. Clearly, this is not the case with MgO increasing much more rapidly than either

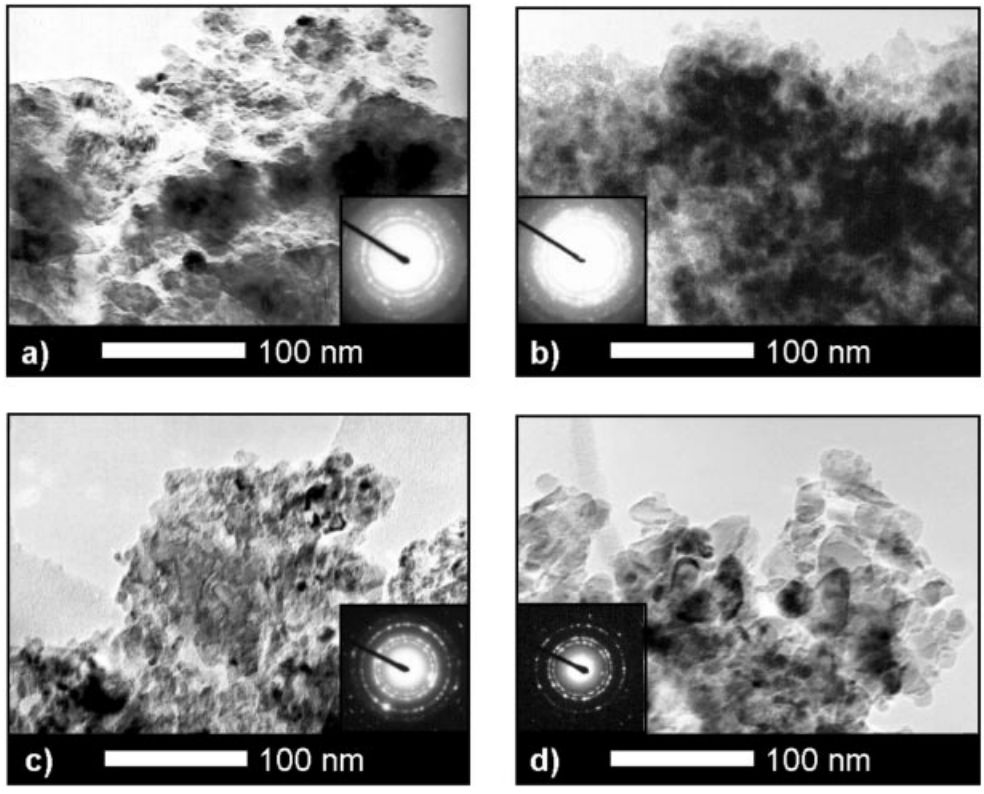

Fig. 3. Transmission electron micrographs and selected area electron diffraction patterns of as-milled and annealed (1 h at 1200°C) powders after leaching for 18 h at room temperature using 3% HCl: (a) rutile milled with nitrogen; (b) ilmenite milled with carbon; (c) rutile milled with carbon then annealed; (d) ilmenite milled with nitrogen then annealed.

TiN or TiC. The phases present are mutually dispersed during milling[42] and coalescence of particles would be hindered. For the ilmenite derived powders the volume fraction of MgO was ~36% whereas in the rutile derived powders the fraction was ~47%, clearly there is significant difference in the expected dispersion of MgO. This is reflected in the powders containing iron showing a somewhat smaller MgO size after annealing than those without iron. There does not seem to be a parallel to this for the hard phases, the crystallite sizes for TiC are smaller than those of TiN regardless of the differences in dispersion (~26 vol% hard phase with iron and ~51 vol% without).

The presence of titanium oxycarbide, TiC_xO_{1-x}, rather than a carbon deficient carbide $TiC_{<1}$ is certain for powders derived from both rutile and ilmenite. The increased unit cell size after annealing is consistent with previously reported results in thermally processed systems.[29,34] In experiments identical to these, but using aluminium instead of magnesium,[13–15] there was no evidence for a oxycarbide phase, presumably this was due to the greater affinity of aluminium for oxygen compared with mg ($\Delta G_{298} = -609\,kJ\,mol^{-1}$ MgO, $\Delta G_{298} = -1690\,kJ\,mol^{-1}$ Al_2O_3). Also, it is known that the removal of small fractions of oxygen from the oxycarbide phase is difficult.[29]

Heating another sample of the ilmenite derived carbide (b) at 1500°C removed the peaks at 51.2° and 59.8° which are indicative of a solid solution of carbon in iron and intensified the elemental iron peak at 52.4°, the titanium carbide peaks also moved to lower 2θ indicating an increase in the unit cell size. Increasing the annealing temperature has been shown[29,34,35] to produce an oxycarbide with an increasing fraction of carbon, which leads to an increase in the d-spacings of the TiC_xO_{1-x} phase.[43] The unit cell size after annealing at 1500°C was 0·43271 nm, equivalent to $TiC_{0.97}$[30] (or $TiC_{0.998}O_{0.002}$), there was no mass loss associated with the reaction implying that reaction (6) had occurred between 1200 and 1500°C.

$$TiC_xO_{1-x} + Fe(yC) + \{1-x\}Mg \Rightarrow Fe + TiC_{x+y} + \{1-x\}MgO \qquad (6)$$

This reaction is consistent with the work of Frage et al.[44,45] who found that carbon would be removed from iron-carbon alloys by interaction with sub-stoichiometric TiC to eventually form $TiC_{0.98}$. Thus it would seem that there was magnesium remaining after milling which was not evident during DTA, this was presumably due to oxidation on exposure to atmosphere after milling.

The formation and separation of hard materials by a room temperature route has potentially major industrial applications with relatively simple processing requirements. The ease of separation of the unwanted phases formed during milling makes the production a two-stage process, milling then leaching. Annealing of the powder prior to leaching produces a larger crystallite and particle size which would make handling the powder somewhat simpler. Also, for the samples milled with graphite, a thermal reaction occurs decreasing the oxygen content of the oxycarbide phase. For both nitride and carbide the apparent yield was greater after annealing than before, with a substantial decrease in dissolution compared with the as-milled powder. Thus, it would seem prudent to anneal the powder after milling to form larger particles, convert the oxycarbide to carbide when iron is present and to decrease the dissolution of the hard phase. However, it has been shown elsewhere[25,37] that milling of a mixture of carbon with either ilmenite or rutile leads to a decrease in the temperature of reaction and an increase in the rate of formation of titanium carbide during thermal processing. Indeed, 100 h milling of a mixture of ilmenite and graphite has shown formation of TiC in 1 h at 1300°C and apparently complete formation of TiN in 1 h at 1100°C,[25,37] substantially more rapidly than 4 h at 1550°C reported for complete conversion to carbide of 20–25 nm TiO_2 particles coated in carbon.[46,47] These powders were composed of impact welded aggregates of polycrystalline particles which were < 500 nm. The present study forms smaller particles that are apparently single crystals and the investigation of lower annealing temperatures for the magnesium reduced powders may prove to have a further economical advantage. A thorough examination of the separation step would probably prove to be valuable with the loss of the smallest crystallites when using hydrochloric acid. An alternative leach reagent, in which the hard phase is less soluble, may well prove to give a greater yield of the desired phases.

A similar system involving magnesium reduction of rutile in the presence of boric oxide[48] showed the reaction occurred suddenly and completely between 10 and 15 h of milling forming TiB_2 and MgO and it may be that the same occurred in the systems examined here. The mill used in these experiments is extremely inefficient and other mills with a greater rate of energy transfer could be expected to produce the same improvements for a much shorter milling time. Mathematical modeling of milling[49–51] has indicated that vibratory mills may be ~1000 times faster than ball mills, a further improvement has been reported for stirred mills.[52] Thus, the same process enhancements as demonstrated for

100 h ball milled samples may be achievable within 10 min by using a different type of mill. This substantial time saving makes this method of producing nanometric hard materials considerably more attractive; however, this improvement has yet to be proven experimentally.

5 Conclusions

Titanium oxycarbide and titanium nitride have been formed at room temperature by mechanochemical reaction between either ilmenite or rutile and magnesium in the presence of carbon or nitrogen. The reaction was apparently complete for the oxycarbide within 100 h but the nitride reaction was incomplete. The XRD crystallite size of the as-milled powders was < 10 nm, but on annealing for 1 h at 1200°C increased to 16–20 nm for all except the carbide derived from ilmenite. The MgO formed during milling was readily removed from the hard material by a simple acid leaching which left porous aggregates of hard material particles. Sonication easily broke up the aggregates and transmission electron microscopy indicated that the particles were of similar size to the XRD crystallite size implying that they were single crystal. Leaching of the powders showed an increased crystallite size indicating that the smaller crystallites were preferentially leaching. The unit cell size of the carbides indicated that an oxycarbide was formed during milling and formation of a carbide phase occurred only on annealing. There was no evidence of any phase, other than nitride, forming in the powders milled in nitrogen.

Acknowledgement

The authors would like to thank Lily Shen of the Electron Microscope Unit at the Australian National University for her substantial aid in producing this paper.

References

1. Welham, N. J., Enhancement of the dissolution of ilmenite ($FeTiO_3$) by extended milling. *Transactions of the Institution of Mining and Metallurgy*, 1997, **106C**, 141–144.
2. Welham, N. J., Formation of micronised WC from scheelite ($CaWO_4$). *Materials Science and Engineering A*, 1998, **248**, 230–237.
3. Welham, N. J., Room temperature reduction of scheelite ($CaWO_4$). *Journal of Materials Research*, 1999, **14**, 619–626.
4. Welham, N. J. and Llewellyn, D. J., Mechanical enhancement of the dissolution of ilmenite. *Minerals Engineering*, 1998, **11**, 827–841.
5. Ding, J., Miao, W. F., McCormick, P. G. and Street, R., Mechanochemical synthesis of ultrafine Fe powder. *Applied Physics Letters*, 1995, **67**, 3804–3806.
6. Ding, J., Tsuzuki, T., McCormick, P. G. and Street, R., Structure and magnetic properties of ultrafine Fe powders by mechanochemical processing. *Journal of Magnetism & Magnetic Materials*, 1996, **162**, 271–276.
7. Ding, J., Tsuzuki, T., McCormick, P. G. and Street, R., Ultrafine Co and Ni particles prepared by mechanochemical processing. *Journal of Physics D Applied Physics*, 1996, **29**, 2365–2369.
8. Ding, J., Tsuzuki, T., McCormick, P. G. and Street, R., Ultrafine Cu particles prepared by mechanochemical process. *Journal of Alloys & Compounds*, 1996, **234**, L1–3.
9. Tsuzuki, T. and McCormick, P. G., Synthesis of CdS quantum dots by mechanochemical reaction. *Applied Physics A–Solids & Surfaces*, 1997, **65**, 607–609.
10. Ding, J., Tsuzuki, T. and McCormick, P. G., Mechanochemical synthesis of ultrafine ZrO_2 powder. *Nanostructured Materials*, 1997, **8**, 75–81.
11. Ding, J., Tsuzuki, T. and McCormick, P. G., Ultrafine alumina particles prepared by mechanochemical/thermal processing. *Journal of the American Ceramic Society*, 1996, **79**, 2956–2958.
12. Welham, N. J., Kerr, A. and Willis, P. E., Ambient temperature mechanochemical formation of titanium nitride from TiO_2 and $FeTiO_3$. *Journal of the American Ceramic Society*, in press.
13. Willis, P. E., Welham, N. J. and Kerr, A., Ambient temperature formation of an alumina–titanium carbide–metal ceramic. *Journal of the European Ceramic Society*, 1998, **18**, 701–708.
14. Kerr, A., Welham, N. J. and Willis, P. E., Low temperature formation of titanium carbonitride. *Nanostructured Materials*, in press.
15. Welham, N. J., Willis, P. E. and Kerr, A., Mechanochemical formation of metal–ceramic composites. *Journal of the American Ceramic Society*, in press.
16. Roine, A., *HSC Chemistry for Windows*. Outokumpu Research Oy, Pori, 1994.
17. Calka, A. and Radlinski, A. P., Universal high performance ball milling device and its application for mechanical alloying. *Materials Science and Engineering*, 1991, **A134**, 1350–1353.
18. Warren, B. E., *X-Ray Diffraction*. Dover, New York, 1990, pp. 251–314.
19. Klug, H. P. and Alexander, L. E., *X-Ray Diffraction Procedures*. John Wiley, New York, 1954 p. 716.
20. Welham, N. J., Mechanically induced reduction of ilmenite ($FeTiO_3$) and rutile (TiO_2) by magnesium. *Journal of Alloys & Compounds*, 1998, **274**, 260–265.
21. Becher, R. G., Canning, R. G., Goodheart, B. A. and Uusna, S., A new process for upgrading ilmenitic mineral sands. *Proceedings of the Australasian Institute of Mining and Metallurgy*, 1965, **214**, 21–44.
22. Grey, I. E., Jones, D. G. and Reid, A. F., Reaction sequences in the reduction of ilmenite: I introduction. *Transactions of the Institution of Mining and Metallurgy*, 1973, **82C**, 151–152.
23. Grey, I. E. and Reid, A. F., Reaction sequences in the reduction of ilmenite: III reduction in a commercial rotary kiln; an X ray diffraction study. *Transactions of the Institution of Mining and Metallurgy*, 1974, **83C**, 39–46.
24. Welham, N. J., A parametric study of the mechanically activated carbothermic reduction of ilmenite. *Minerals Engineering*, 1996, **9**, 1189–1200.
25. Welham, N. J. and Willis, P. E., Direct synthesis of TiC/TiN–Fe composites from ilmenite concentrate. *Metallurgical and Materials Transactions B*, 1998, **29**, 1077–1083.
26. White, G. V., MacKenzie, K. J. D. and Johnston, J. H., Carbothermal synthesis of titanium nitride Part I. Influence of starting materials. *Journal of Materials Science*, 1992, **27**, 4287–4293.

27. White, G. V., MacKenzie, K. J. D., Brown, I. W. M., Bowden, M. E. and Johnston, J. H., Carbothermal synthesis of titanium nitride Part II. The reaction sequence. *Journal of Materials Science*, 1992, **27**, 4294–4299.
28. White, G. V., MacKenzie, K. J. D., Brown, I. W. M. and Johnston, J. H., Carbothermal synthesis of titanium nitride Part III. Kinetics and mechanism. *Journal of Materials Science*, 1992, **27**, 4300–4304.
29. Storms, E. K., *The Refractory Carbides*. Academic Press, New York, 1967 pp. 1–17.
30. Albertsen, K. and Schaller, H. J., Constitution and thermodynamics of the system Ti–C. *Zeitschrift fur Metallkunde*, 1995, **86**, 319–325.
31. Tristant, P. and Lefort, P., Approche cinétique de la réduction carbothermique du dioxyde de titane. *Journal of Alloys & Compounds*, 1993, **196**, 137–144.
32. Afir, A., Achour, M. and Pialoux, A., Etude de la reduction carbothermique du dioxyde de titane par diffraction X à haute température sous pression contrôlée. *Journal of Alloys & Compounds*, 1994, **210**, 201–208.
33. Terry, B., Azubike, D. C. and Chrysanthou, A., Reduction/carburisation of columbite concentrate. *Scandinavian Journal of Metallurgy*, 1994, **23**, 130–136.
34. Terry, B. S. and Chinyamakobvu, O., Carbothermic reduction of ilmenite and rutile as means of production of iron based Ti(O,C) metal matrix composites. *Materials Science and Technology*, 1991, **7**, 842–848.
35. Coley, K. S., Terry, B. S. and Grieveson, P., Simultaneous reduction and carburization of ilmenite. *Metallurgical and Materials Transactions B*, 1995, **26**, 485–494.
36. ICDD, *Powder Diffraction File*, 1996 (up to set 46).
37. Welham, N. J., Carbothermic reduction of ilmenite and rutile. *Metallurgical Transactions*, submitted for publication.
38. Welham, N. J., Ambient temperature formation of (Ta,Nb)C and (Ta,Nb)N. *Journal of Materials Science*, 1999, **34**, 1–7.
39. Welham, N. J., Non thermal production of tungsten from scheelite. *Materials Science and Technology*, 1999, **15**, 456–458.
40. Milosev, L., Strehblow, H. H., Navinsek, B. and Metikoshukovic, M., Electrochemical and thermal oxidation of TiN coatings studied by XPS. *Surface & Interface Analysis*, 1995, **23**, 529–539.
41. Bauer, A. D., Herranen, M., Ljungcrantz, H., Carlsson, J. O. and Sundgren, J. E., Corrosion behaviour of monocrystalline titanium nitride. *Surface & Coatings Technology*, 1997, **91**, 208–214.
42. Welham, N. J., Mechanical activation of the solid-state reaction between Al and TiO_2. *Materials Science and Engineering A*, 1998, **255**, 81–89.
43. Pivovarov, L. K., Vrzheshch, E. Y., Kreimer, G. S. and Zakirov, F. G., Vacant sites in the crystal lattice of TiC–TiO solid solutions. *Russian Journal of Inorganic Chemistry*, 1967, **12**, 917–919.
44. Frage, N., Levin, L., Manor, E., Shneck, R. and Zabicky, J., Iron–titanium–carbon system. 1. Equilibrium between titanium carbide (TiC_x) of various stoichiometries and iron–carbon alloys. *Scripta Materialia*, 1996, **35**, 791–797.
45. Frage, N., Levin, L., Manor, E., Shneck, R. and Zabicky, J., Iron–titanium–carbon system. 2. Microstructure of titanium carbide (TiC_x) of various stoichiometries infiltrated with iron–carbon alloy. *Scripta Materialia*, 1996, **35**, 799–803.
46. Koc, R., Kinetics and phase evolution during carbothermal synthesis of titanium carbide from ultrafine titania/carbon mixture. *Journal of Materials Science*, 1998, **33**, 1049–1055.
47. Koc, R., Kinetics and phase evolution during carbothermal synthesis of titanium carbide from carbon-coated titania powder. *Journal of the European Ceramic Society*, 1997, **17**, 1309–1315.
48. Welham, N. J., Room temperature formation of TiB_2 from oxides. *Minerals Engineering*, in press.
49. Heegn, H., On the connection between ultrafine grinding and mechanical activation of minerals. *Aufbereitungs-Technik*, 1989, **30**, 635–642.
50. Tkacova, K., Heegn, H. and Stevulova, N., Energy transfer and conversion during comminution and mechanical activation. *International Journal of Mineral Processing*, 1993, **40**, 17–31.
51. Maurice, D. and Courtney, T. H., Milling dynamics. 2. Dynamics of a spex mill and a one-dimensional mill. *Metallurgical & Materials Transactions A*, 1996, **27**, 1973–1979.
52. Warris, C. J. and McConnick, P. G., Mechanochemical processing of refractory pyrite. *Minerals Engineering*, 1997, **10**, 1119–1125.